The Subcallosal Cingulate Gyrus in the Context of Major Depression

Clement Hamani, Helen Mayberg, Scellig Stone, Adrian Laxton, Suzanne Haber, and Andres M. Lozano

The subcallosal cingulate gyrus (SCG), including Brodmann area 25 and parts of 24 and 32, is the portion of the cingulum that lies ventral to the corpus callosum. It constitutes an important node in a network that includes cortical structures, the limbic system, thalamus, hypothalamus, and brainstem nuclei. Imaging studies have shown abnormal SCG metabolic activity in patients with depression, a pattern that is reversed by various antidepressant therapies. The involvement of the SCG in mechanisms of depression and its emerging potential role as a surgical target for deep brain stimulation has focused recent interest in this area. We review anatomic and histologic attributes of the SCG and the morphologic and imaging changes observed in depression. Particular attention is given to the regional and downstream structures that could be influenced by the application of deep brain stimulation in this region.

Key Words: Brodmann area 25, cingulate gyrus, cingulum, corpus callosum, deep brain stimulation, depression, prefrontal cortex, psychiatry

There has been a marked increase in the number of clinical conditions treated with deep brain stimulation (DBS). Among the most promising indications are psychiatric disorders, particularly major depression (1–7). We have recently targeted the subcallosal cingulate gyrus (SCG) and adjacent white matter (2,4) based on preliminary imaging data, showing an involvement of this region in the mechanisms of treatment-resistant depression (8,9). The growing interest in this area (8–10) and its emerging potential role as a surgical target for DBS (2,4), warranted a review of histologic and anatomic aspects of the subcallosal cingulum in the context of depression.

Anatomy, Subdivision, and Histology of the Subgenual Portion of the Cingulate Gyrus

The Cingulate Gyrus

The cingulate gyrus is an arch-shaped convolution in the medial surface of the cerebral hemisphere. It lies in close relation to the corpus callosum, from which it is separated by the callosal fissure (11). It commences below the rostrum, curves around anterior to the genu, extends along the dorsal surface of the body, and finally turns ventrally behind the splenium, where it is connected by a narrow isthmus with the hippocampal gyrus (11). It is separated from the medial part of the superior frontal gyrus by the cingulate sulcus, which commonly extends posteriorly into the parietal lobe as the marginal ramus.

On the basis of cytoarchitectural characteristics (discussed subsequently), the cingulate gyrus has been classically subdivided in anterior cingulate cortex (ACC), posterior cingulate cortex, and retrosplenial cingulate cortex (12–14). Alternatively, it has been subdivided in four main regions based not only on histologic features but also common afferent and efferent projections (15–17). These are the anterior cingulate cortex (further subdivided in subgenual ACC [sACC] and paragenual ACC [pACC] regions), midcingulate cortex, posterior cingulate cortex, and retrosplenial cortex (15,16). Here we review one subcomponent of the anterior cingulate gyrus, the SCG. This is operationally defined here as the portion of the cingulate gyrus lying ventral to the corpus callosum, from the anterior boundary of the genu to the rostrum. In this context, the terms *SCG* and *subgenual cingulum* may be used as synonyms. Comprehensive reviews on the anatomic and physiologic aspects more dorsal regions of the ACC have been published elsewhere (12,13,15).

The Anterior Cingulate Gyrus and the Subcallosal Cingulum

According to Brodmann's classification (14), the ACC in humans comprises areas 24, 25, 32 (Figure S1 in Supplement 1) and 33 (not represented in the figure; details follow). Regions of the cingulate cortex lying ventral to the corpus callosum include area 25 and the subcallosal portions of 32 and 24 (Figure S1A in Supplement 1). Although the SCG in nonhuman primates also comprises area 25 and portions of 24 and 32, differences exist across species. In contrast to more traditional studies, recent reports in humans suggest that Brodmann's area (BA) 32 may be subdivided in two: a ventral portion located in the vicinity of BA25 and a dorsal portion located anterior and dorsal to the corpus callosum (18). The former has been suggested as the homologous of the prelimbic BA32 in nonhuman primates. To date, correspondence between cortical regions in nonhuman primates and humans remains controversial. Future investigation is still needed to address this issue.

In nonhuman primates and humans, the ACC subdivisions undergo a progressive differentiation (14,16,19–21). Areas 25 and 32 have poorly differentiated Layers II and III, no layer IV, a prominent Layer V, and a relatively thin Layer VI (14,16,19–21). Area 24 is also characterized by the absence of Layer IV and relatively poorly differentiated Layers II and III. Its Layer V, however, contains large pyramidal neurons and may be subdivided in Layers Va and Vb. Layer VI is well developed (14,16,19–21). Cytoarchitectonically, area 24 may be subdivided in three main regions progressively more differentiated from ventral to dorsal. Area 24a borders the indusium griseum and has been described as periallocortex. Area 24b is more differentiated and considered proisocortex. Area 24c lies within the depths of the cingulate sulcus (14). Area 33 only appears in humans and is located within the depths of the callosal sulcus surrounding the rostrum of the corpus callosum (14). It contains moderate size cells in Layers II and III and heavily stained neurons in Layer V.

In nonhuman primates, the mean number of cells per cubic millimeters in the ACC is approximately 55,000 with no significant differences across BA 25, 24, and 32 (22,23). Although most of these cells are thought to be glutamatergic, approximately 25% comprise gamma-aminobutyric acid (GABA)ergic local circuit neurons (22). GABAergic neurons are mainly distributed in Layers II and III but are

From the Division of Neurosurgery (CH, SS, AL, AML), Toronto Western Hospital, University of Toronto, University Health Network; Section of Neuroimaging (CH), Centre for Addiction and Mental Health, Toronto, Canada; Departments of Psychiatry and Neurology (HM), Emory University School of Medicine, Atlanta, Georgia; and Department of Neurobiology and Anatomy (SH), University of Rochester, Rochester, New York.

Address correspondence to Clement Hamani, M.D., Ph.D., Division of Neurosurgery, Toronto Western Hospital, Toronto, ON M5T 2S8, Canada; E-mail: Clement.Hamani@uhn.on.ca.

Received Apr 25, 2010; revised Aug 16, 2010; accepted Sep 2, 2010.

0006-3223/$36.00
doi:10.1016/j.biopsych.2010.09.034

also found in Layers V and VI (22). In nonhuman primates and humans, 5% to 12% of ACC neuronal populations express calretinin, parvalbumin, and calbindin (22,24).

When neurotransmitter receptors are considered, autoradiography studies in postmortem human brains indicate that the ACC is not homogeneous. When compared with neighbor regions, BA25 has low $GABA_B$, high *N*-methyl-D-aspartate, and high $5\text{-}HT1_A$ (serotonin 1 A) receptor densities, more closely resembling the midcingulate cortex (25).

Projections to and from the Subcallosal Cingulum

In nonhuman primates, studies on SCG projections have mainly characterized afferents and efferents to and from BA25 (Figure 1). BA32 projections have been predominantly studied in regions anterior and dorsal to the SCG (e.g., prelimbic BA32). Because the prelimbic BA32 in nonhuman primates has been suggested to be homologous to the subgenual BA32 in humans, afferent and efferent projections to and from this region are reported later in the article (26). SCG BA24 projections in nonhuman primates have not been characterized in detail.

Afferents to BA25

In nonhuman primates, the most prominent frontal cortical projections to BA25 originate from the orbitofrontal cortex (areas 11 and 13a), medial prefrontal cortex (areas 10 m, 14, 32, 24, and 23), and agranular insula (18,26–30). Projections from the temporal lobe arise from auditory association areas (20) and the temporal pole (31,32). Mesial temporal lobe afferents originate from the subiculum, hippocampal CA1 region (33,34), and amygdala (lateral, basal, and accessory basal nuclei) (35,36). In addition, BA25 also receives projections from the entorhinal and parahippocampal cortices (37,38).

Thalamic afferents to BA25 in nonhuman primates originate from the parvocellular division of the mediodorsal nucleus (MD), paratenial nucleus (PT), and nucleus reuniens (Re) but also the from anteromedial, central lateral, parafascicular, and limitans nuclei (21,39,40). Hypothalamic projections to BA25 arise in posterior, dorsal, and lateral hypothalamic areas (41,42). The main brainstem projections to the ventral medial prefrontal cortex in nonhuman primates are from the ventral tegmental area (VTA) and raphe (43,44).

Efferents from BA25

Cortical efferents from BA25 in nonhuman primates innervate mainly the temporal pole, agranular insula, orbitofrontal cortex (areas 14c, 14r, and 10 m), and areas 32 and 24 (28).

Subcortical projections penetrate the adjacent white matter and innervate rostral and medial aspects of the caudate nucleus, nucleus accumbens (mainly the shell), medial preoptic area, bed nucleus of the stria terminalis, diagonal band of Broca, and lateral septum (45–48). Thereafter, projections from BA25 run caudally through the substantia innominata to innervate the amygdala and parts of the hypothalamus (45,46). Within the amygdala, axons terminate mainly in the intercalated nuclei and parvocellular portion of the basal nucleus. In addition, the intermediate nucleus, magnocellular part of the basal nucleus, periamygdaloid cortex, and, to a lesser extent, the lateral and central nuclei also receive projections from BA25 (45,46).

In nonhuman primates, efferents to the thalamus primarily innervate the magnocellular division of MD, PT, paraventricular nucleus (PV), and Re (40,45,46), but also the reticular, interanteromedial, central medial, parafascicular, and the limitans nuclei (45,46). In the hypothalamus, fibers from BA25 innervate the medial preoptic area (45,46,49), the perifornical region, tuberomammilary nucleus, and posterior hypothalamic area. Projections reaching the posterior third of the hypothalamus arborize through the rostrocaudal extent of the periaqueductal gray matter (PAG). Fibers running through the lateral hypothalamic area travel caudally to innervate the VTA, retrorubral field, substantial nigra compacta, pedunculopontine nucleus, cuneiform nucleus, parabrachial nucleus, raphe, and locus coeruleus (45,46).

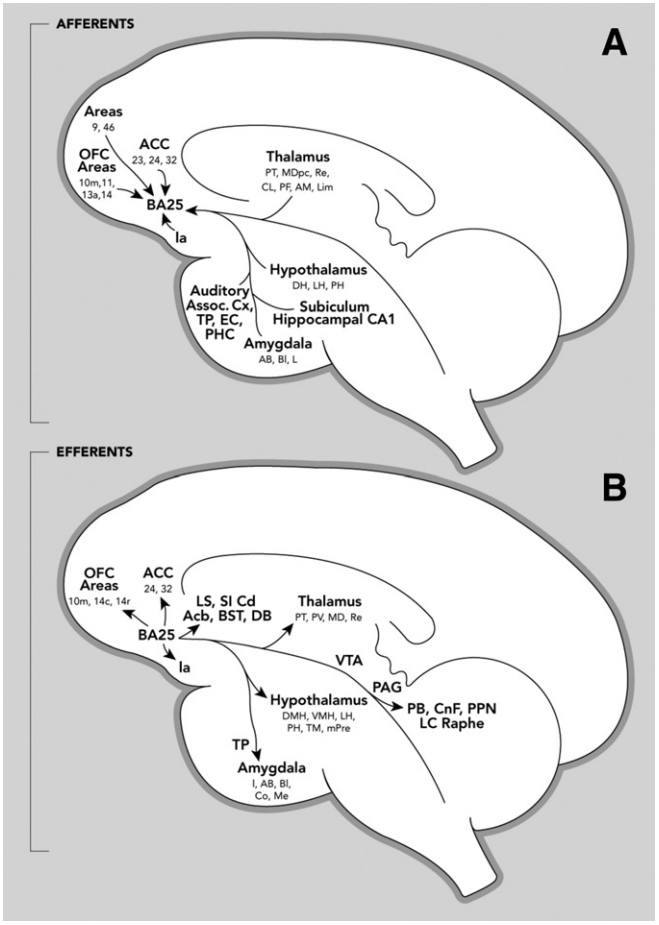

Figure 1. Schematic diagram illustrating the main afferent **(A)** and efferent **(B)** projections from and to Brodmann area 25 in nonhuman primates. Acb, nucleus accumbens; ACC, anterior cingulate cortex; amygdala (AB, accessory basal nucleus; Bl, basolateral nucleus; Co, cortical nucleus; I, intercalated nucleus; L, lateral nucleus; Me, medial nucleus); BST, bed nucleus of the stria terminalis; Cd, caudate nucleus; CnF, cuneiform nucleus; DB, diagonal band of Broca; EC, entorhinal cortex; hypothalamus (DH, dorsal hypothalamus; DMH, dorsomedial hypothalamus; LH, lateral hypothalamus; PH, posterior hypothalamus; Mpre, medial preoptic area; TM, tuberomammillary nucleus; VMH, ventromedial hypothalamus); Ia, agranular insular cortex; LC, locus coeruleus; LS, lateral septal nucleus; OFC, orbitofrontal cortex; PAG, periaqueductal gray; PB, parabrachial nucleus; PHC, parahippocampal cortex; PPN, pedunculopontine nucleus; SI, substantia innominata; TP, temporal pole; thalamus (AM, anteromedial nucleus; MD, mediodorsal nucleus; MDpc, parvicellular portion of the mediodorsal nucleus; PT, paratenial nucleus; Re, nucleus reuniens; CL, central lateral nucleus; lim, nucleus limitans; PF, parafascicular nucleus; PV, paraventricular nucleus); VTA, ventral tegmental area (portions of this figure were modified and reprinted [45], with permission from Elsevier, Copyright 2001).

Afferents to BA32

Similar to projections described for BA25, cortical projections to BA32 in nonhuman primates originate mainly from the orbitofron-

tal cortex, medial prefrontal cortex (areas 10, 11, 12, 14, 24, 25), agranular insula, and temporal pole (18,26–28,31). Mesial temporal lobe afferents arise from the amygdala (basal nuclear complex) (35,36) and the entorhinal and parahippocampal cortices (37,50). Thalamic afferents to BA32 originate primarily from MD, PT, and PV (38,40,51), whereas both anterior and posterior hypothalamic areas projects to this cortical region (49).

Efferents from BA32

Cortical efferents from BA32 in nonhuman primates predominantly innervate the agranular insula, orbitofrontal and medial prefrontal cortical regions (areas 12, 10, 11, 14, and 24) (28,45), the temporal pole (31,45), entorhinal cortex, piriform cortex (45), and parahippocampal gyrus (37,45).

Subcortical projections innervate ventromedial aspects of the caudate nucleus, the nucleus accumbens (45,48,52), ventral putamen (52), the diagonal band of Broca, lateral septum, and substantia innominata (45). Within the amygdala, BA32 efferents terminate in the basolateral nucleus, basomedial nucleus (36,45), accessory basal nucleus, and lateral nucleus (45). In nonhuman primates, efferents to the thalamus primarily innervate the MD, PT, and PV (38,40,45,50) but also Re, reticular nucleus, limitans nucleus, and parts of the pulvinar (45). In the hypothalamus, fibers from BA32 innervate the lateral preoptic nucleus, dorsal medial nucleus, ventral medial nucleus, lateral hypothalamic nuclei, posterior hypothalamic nuclei, and the tuberomammillary nucleus (45,49). In the brainstem, BA32 projects to the PAG (53), pedunculopontine nucleus, dorsal raphe (45), VTA (45,54), and substantial nigra compacta (54).

Subcallosal Cingulum and Depression

When healthy subjects are asked to rehearse autobiographic sad scripts or are depleted of tryptophan, cerebral blood flow increases in the SCG (Figure 2) (9,55–58). In patients with depression, imaging studies have often shown an increased SCG activity (4,59–61). This has been sometimes reported in association with a reduced activity in BA 46/9 (8–10). A decrease in SCG activity has been observed after treatment with a variety of interventions, including antidepressants, DBS, electroconvulsive therapy, repetitive transcranial magnetic stimulation, cingulotomy, and placebo (Figure 2) (4,8–10,59,62–65).

Volumetric Studies

The hippocampus and prefrontal cortex bear significant morphologic alterations in depression (66–70). As an example, the subgenual area 24 of patients with familial mood disorders have a 35% volumetric reduction (71) and 24% to 41% fewer glial cells than control samples (Figure 2) (68,71). This is of considerable importance in light of recent experiments showing that 1) the inactivation of glia in the medial prefrontal cortex induces depressive-like behaviors in rats (72,73) and 2) medial prefrontal cortex glial cell proliferation has been suggested as one of the mechanisms of action of electroconvulsive therapy in rodents (74,75).

Imaging studies conducting volumetric magnetic resonance imaging assessments of the SCG in depression are more controversial. A series of reports including common authors have shown that the cortical volume of the SCG was reduced in patients with familial depression (60), women with early-onset depression (76), and patients with psychotic depression (77). Although these findings have been replicated by some investigators (78), they were not corroborated by others (79). Apart from technical factors in data acquisition and analysis, potential explanations for such discrepancies include disease severity and genetic factors. Brambilla and colleagues (79) have suggested that patients with severe depression had a greater SCG volumetric reduction compared with those with mild forms of the disease. Pezawas and colleagues (80) have shown a reduced SCG gray matter volume in healthy subjects with the short allele of the serotonin transporter gene (Figure 2). This is of interest because these individuals seem to have an increased risk of developing depression compared with those with the long allele.

SCG Projections and the Clinical Features of Depression

It is clear that depression is multi-symptomatic with disturbances in cognitive, somatic, vegetative, mood, and behavioral domains. As a consequence of its extensive connections, the disrupted function of the SCG may influence structures involved in the pathophysiology of the constellation of observed depressive symptoms. Projections to prefrontal cortical areas may interfere with executive and cognitive processes. Those to the nucleus accumbens could play a role in the lack of interest and disruption of reward mechanisms and underlie anhedonia. Projections to the hypothalamus and brainstem could disrupt normal drive and vegetative function, leading to circadian and sleep disturbances (81), problems with appetite, and abnormalities in stress response and cortisol metabolism. Projections to the PAG could interfere with the normal perception or processing of pain.

The amygdala is another key region linked to the pathophysiology of depression. Glucose metabolism and blood flow are increased in the amygdala of depressed patients, a pattern that is reversed by antidepressants (82,83). Pezawas and colleagues (80)

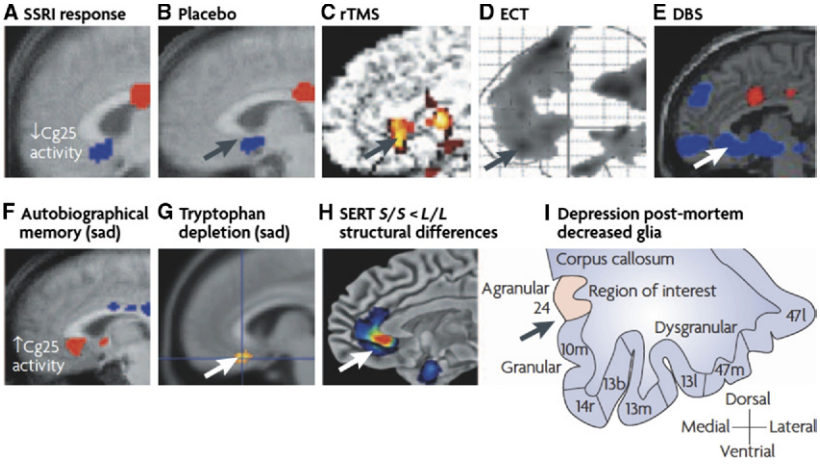

Figure 2. Common imaging pattern of subgenual cingulate gyrus, glucose metabolic or blood flow reduction to various antidepressant interventions. Images demonstrate group change patterns relative to baseline depressed states for each treatment response to a **(A)** serotonin reuptake inhibitor (SSRI), **(B)** placebo, **(C)** repetitive transcranial magnetic stimulation (rTMS), **(D)** electroconvulsive therapy (ECT), and **(E)** high-frequency deep brain stimulation (DBS). Common pattern of subgenual cingulate gyrus blood flow increases with induction of transient sadness induced by both recollection of a personal sad memory **(F)** and tryptophan depletion in healthy subjects **(G)**. Anatomic differences in SCG distinguish healthy subjects homozygous for the *S* allele of the serotonin transporter promoter gene (a putative risk factor for depression) relative to *L/L* carriers **(H)**. Area of decreased glial number in postmortem studies of depressed patients relative to nondepressed subjects **(I)**. Reprinted by permission from Macmillan Publishers Ltd: *Nature Reviews Drug Discovery* (97), Copyright 2007.

have recently shown with functional MRI that activity in subgenual cortical regions correlates positively with activity in the amygdala when subjects are presented with threatening faces. In this context, the coupling of these structures might be relevant in the circuitry of the disease. Finally, SCG projects to the entorhinal cortex and parahippocampal gyrus, which connect extensively with the hippocampus. Through these projections cognitive and memory function may be influenced.

Subcallosal Deep Brain Stimulation

In other applications of DBS (i.e., movement disorders), the clinical effects of high-frequency stimulation mimic those observed with lesions. Bearing this in mind, the initial premise was that high-frequency stimulation of the SCG could disrupt pathologic activity and reverse the metabolic pattern observed in depression (4,8,9,84).

To date, the outcome of 20 patients with depression treated with SCG DBS has been reported. At 1 year, 11 (55%) responded to surgery with a greater than 50% reduction in 17-item Hamilton Depression Scale scores. Seven patients (35%) achieved or were within 1 point of achieving remission (scores < 8) (2). Of note, patients who responded to surgery had a significant improvement in mood, anxiety, sleep, and somatic complains related to the disease (2). Also important was the safety of the procedure, with no serious permanent adverse effects (2) or changes in neuropsychological profile recorded (85). As previously shown, pretreatment metabolic changes assessed with positron emission tomography were reversed in patients who improved after DBS (2,4). Structures influenced by stimulation in our study were predominantly those receiving SCG projections (e.g., medial regions of the prefrontal cortex, orbitofrontal cortex, hypothalamus, PAG, thalamus, nucleus accumbens, posterior regions of the cingulate gyrus, among others) (2,4). This suggests that modulation of a distributed set of regions defined by anatomic connections might mediate the antidepressant effects of SCC DBS, rather than local changes restricted to the target. It also suggests that additional effects may be facilitated by transsynaptic changes in brain regions indirectly connected to areas receiving SCG projections (e.g., dorsolateral prefrontal cortex, insula).

As new clinical, imaging and electrophysiologic studies are conducted, we expect to establish specific attributes for a clinical response. In this same line, we hope to characterize the depressive symptoms more responsive to DBS and perhaps be able to predict which patients are more likely to improve. Blinded clinical trials comparing the outcome of patients assigned to receive active or sham stimulation are ongoing. This will be of particular interest to assess a more definitive role of stimulation for the treatment of depression.

Also important to study potential mechanisms for the antidepressant effects of DBS will be the use of animal models. In a recent series of studies, we have shown that stimulation of the ventromedial prefrontal cortex (vmPFC) at parameters approximating those used in clinical practice induced a significant antidepressant-like response in the forced swim test (FST) in rats (86,87). In rodents as in humans, DBS has been shown to influence the activity of local neuronal populations and remote structures (88,89). This later has been hypothesized to be due to the modulation of fiber tracts nearby the electrodes (for a review, see Lozano *et al.* [89]). To explore whether vmPFC inactivation was responsible for our results, we treated different groups of animals undergoing the FST with radiofrequency lesions, local ibotenic acid (IBO), or muscimol injections (87). IBO is a neuronal toxin, and muscimol is a GABAergic agonist. We found that some of these treatments were somewhat effective in the FST (87), a finding that has been recently corroborated by others (90). In our study, however, the magnitude of response to DBS was more pronounced than that observed after muscimol injections or RF lesions. This suggests that although target inactivation might have played a role in the antidepressant-like effects of vmPFC DBS, it was likely not the sole mechanism. To explore whether fiber pathways near the electrodes were involved in the stimulation response, we took advantage of the selective pattern of IBO lesions (e.g., this neuronal toxin largely preserves fiber pathways at the site of the lesions). We treated a group of rats with vmPFC and IBO in the same target and noticed that the antidepressant-like effects of stimulation were preserved in these animals. Results from this study suggest that IBO-spared fibers might have been involved in the antidepressant-like effects of stimulation in the FST (87). We have then explored whether catecholaminergic systems were involved in mechanisms of DBS. Strikingly, we found that response to stimulation was completely abolished after serotonergic, but not noradrenergic, depleting lesions (87). In addition, at settings that improved behavior, vmPFC DBS induced a significant and prolonged release of hippocampal serotonin (5-HT) (87). Although our results do not necessarily imply that the antidepressant-like effects of vmPFC in the FST were due to an increase in 5-HT release, they do suggest that the integrity of the serotonergic system may be necessary for the efficacy of DBS in rats. Despite these insights, one must always to be cautious when translating data from rodents to humans. Anatomic differences across species, limitations of the FST as a model of depressive states, and the treatment of naive rats in our studies versus refractory depressed patients in clinical trials are only a few of the variables that need to be taken into account (91).

What Structures Are Being Stimulated? The Subcallosal Cingulate Region

Clinically used stimulating electrode contacts in our series were located in an area that extends beyond the subcallosal cingulate cortex (Figure 3) (92). Because the cingulum was not the only structure being stimulated (Figure 3), it is probably more appropriate to consider the procedure as "subcallosal region" (SCR) rather than subcallosal cingulate gyrus or BA25 DBS. As defined here, the SCR is an operational region containing local cortical areas and fiber bundles potentially influenced by stimulation. Its boundaries are the anterior aspect of the genu and posterior portion of the rostrum of the corpus callosum in the anteroposterior plane (Figure 4A), the inferior aspect of the corpus callosum and the most ventral sulcus of the medial frontal lobe in the dorsal ventral plane (Figure 4A and 4B), and the medial edge of the frontal lobe and the upward projection of the olfactory sulcus in the mediolateral plane (Figure 4B).

As previously mentioned, it is well recognized that DBS exerts both local and distant effects by influencing neural elements and axonal projections nearby the electrodes (89,93). In this context, it is relevant to define cortical regions and fiber bundles of the SCR. According to Ongur and colleagues, the prefrontal cortex underneath the corpus callosum in humans may be subdivided in three cytoarchitectonic regions (Figure S2 in Supplement 1) (18): a granular zone (area 10m), a caudoventral agranular zone (BA25 and prelimbic BA32 [32pl]), and a rostrodorsal agranular zone (subgenual BA24 and the dorsal anterior BA32 [32ac]) (18). Bearing in mind the location of the electrode contacts in our series (Figure 3), it likely that stimulation influenced not only BA25, BA24, and BA32pl but also area 10m.

The anatomy of subcallosal fiber systems in humans has not been studied in detail. In nonhuman primates, major fiber pathways include the callosal bundle, the uncinate fascicle, and the

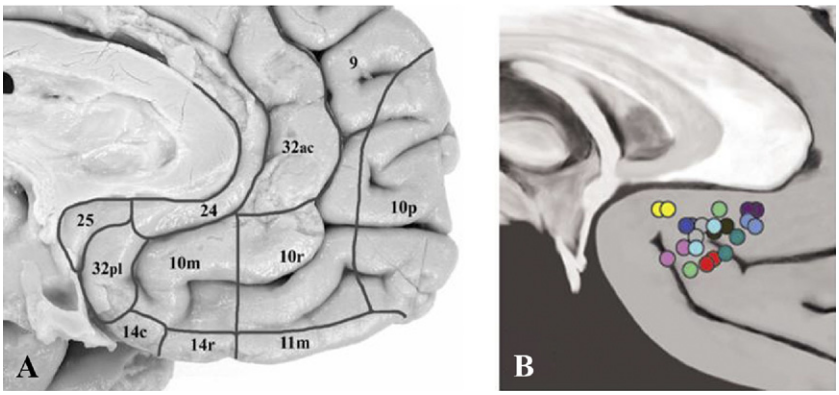

Figure 3. Anatomic regions potentially influenced by deep brain stimulation of the subcallosal region. **(A)** Architectonic subdivision of the medial surface of the human brain according to Ongur and colleagues (reprinted from [18] with permission from John Wiley and Sons). **(B)** Location of deep brain stimulation electrodes in patients with depression who responded to surgery in our series. Note that contacts used for chronic stimulation (colored circles) were clustered in the subcallosal region, not only in cingulate areas 25, 24, and 32pl but also 10m (reprinted from the *Journal of Neurosurgery* [92], with permission from the AANS).

subcortical fascicle (94). The former runs within the depths of the cingulate gyrus, arching around the genu and the splenium. It provides a path that interconnects different regions of the cingulum with its caudal fibers innervating the parahippocampal gyrus, the retrosplenial area in the banks of the calcarine sulcus, and the caudal part of the presubiculum (94). Fibers from the uncinate fascicle and association systems interconnect posterior aspects of the subcallosal region, including BA25, and the amygdala. The subcortical fascicle in nonhuman primates is a fiber bundle through which parts of the medial prefrontal cortex innervate subcortical regions. In humans, with the subdivision of BA32 in areas 32pl and 32ac and the emergence of area 10m, fibers crossing the subcallosal region may differ from those in nonhuman primates.

Projections potentially modulated by DBS in patients with depression have been recently studied with probabilistic tractography (95,96). Two tract patterns within the region of interest were identified, segregating the pregenual (pACC) and sACC. Common to both tract maps were connectivity with the midcingulate cortex, the frontal pole, hypothalamus, and nucleus accumbens. Major differences were that the pACC connected more strongly with the dorsal cingulum, whereas the sACC had stronger connections with subcortical (nucleus accumbens and hypothalamus) and medial temporal lobe structures (amygdala and hippocampus) (95).

Also to be taken into account is the gyral pattern of the subgenual region and the potential influence of DBS on local white matter fibers. In humans, this can be variable but two distinct gyri are often observed (Figure 4). In the example provided, electrode contacts could be implanted in such a way to influence the white matter bundles of each specific gyrus (Figure 4). Variations in gyral anatomy and in electrode position in the SCR could thus have an impact on the neural pathways modulated by stimulation and, in turn, on the behavioral and clinical consequences of DBS. To date, we have not found a correlation between the location of stimulating electrodes within the SCR and outcome in patients with depression (92). Refinement of target selection will require the analysis of more patients with a wider variation in electrode location or the assessment of the effects of stimulation though electrodes specifically implanted over pathways that course in this region.

Summary and Future Perspectives

Imaging studies in patients with depression have shown an increased SCG activity that may be reversed by several antidepressants therapies. As a result, the SCG has been suggested as an important structure in the pathophysiology of depression. Although still investigational, the use of DBS as a therapy for major depression offers a unique opportunity to gain further insight on the physiology of the SCG and its involvement in mechanisms of the disease. As an example, some centers conduct microelectrode recording mapping during surgery. This opens the possibility of characterizing the physiology of SCG neurons in humans while surgeons identify the best electrode implant target. In a homologous scenario, cell recordings conducted during surgical procedures in patients with movement disorders were crucial for our understanding of the physiology of the basal ganglia and the mechanisms of diseases such as Parkinson's, dystonia, and tremor. In addition to microelectrode mapping, patients with electrodes implanted may be stimulated or have local field potentials recorded. This may not only lead to the characterization of predictors of a response to DBS but also increase our understanding of oscillatory patterns and characteristic electrophysiologic features and functions of the SCG. Also of importance will be the contribution of

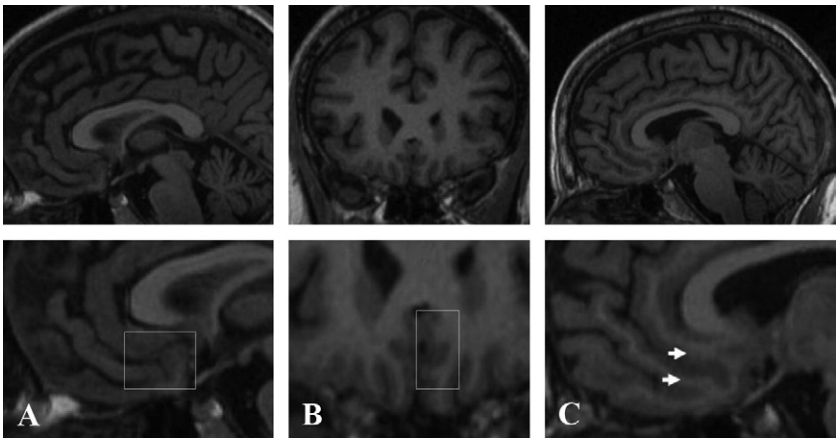

Figure 4. Operational boundaries of the subcallosal region. Sagittal **(A and C)** and coronal **(B)** magnetic resonance images of the brain (top row) with respective magnifications shown in the bottom row. In panels A and B, boxes represent the boundaries of the subcallosal region. In the anteroposterior axis, these are the anterior aspect of the genu and the posterior aspect of the rostrum of the corpus callosum. In the dorsal ventral plane, the subcallosal region extends from the inferior aspect of the corpus callosum to the most ventral sulcus of the medial frontal lobe. Mediolaterally, it extends from the medial edge of the frontal lobe to the upward projection of the olfactory sulcus. Panel C is an example of a patient with two distinct subcallosal region gyri (arrows). Placement of electrodes in each of these might, in theory, influence different white matter bundles, which could subsequently lead to differences in outcome.

imaging modalities. Before surgery, patients may be studied with diffusion tensor imaging, functional MRI, and positron emission tomography. These data sets might be merged with postoperative computed tomography and magnetic resonance images (provided safety specifications for image acquisition are followed), and the correlation among electrode position, physiologic effects, and clinical consequences can be studied. This will not only increase our knowledge of the physiologic attributes of specific anatomic structures, fiber pathways, or metabolically active regions nearby the SCG but also characterize whether any of those could be used to guide placement of the electrodes more effectively for an optimal antidepressant response.

Clinical work by the authors was carried out in part with support from the National Alliance for Research on Schizophrenia and Depression, Stanley Foundation, Woodruff Fund, and Dana Foundation. Animal work was supported in part by National Alliance for Research on Schizophrenia and Depression and Ontario Mental Health Foundation.

Drs. Mayberg and Lozano consult to St. Jude Medical, which has licensed their intellectual property related to deep brain stimulation for depression. Dr. Lozano is a consultant to Medtronic and Boston Scientific. Dr. Hamani is a consultant to St. Jude Medical. Dr. Haber has received honoraria from Medtronic and Eli Lilly. All other authors report no biomedical financial interests or potential conflicts of interest.

Supplementary material cited in this article is available online.

1. Jimenez F, Velasco F, Salin-Pascual R, Hernandez JA, Velasco M, Criales JL, *et al.* (2005): A patient with a resistant major depression disorder treated with deep brain stimulation in the inferior thalamic peduncle. *Neurosurgery* 57:585–593; discussion: 585–593.
2. Lozano AM, Mayberg HS, Giacobbe P, Hamani C, Craddock RC, Kennedy SH (2008): Subcallosal cingulate gyrus deep brain stimulation for treatment-resistant depression. *Biol Psychiatry* 64:461–467.
3. Malone DA Jr, Dougherty DD, Rezai AR, Carpenter LL, Friehs GM, Eskandar EN, *et al.* (2008): Deep brain stimulation of the ventral capsule/ventral striatum for treatment-resistant depression. *Biol Psychiatry* 65: 267–75.
4. Mayberg HS, Lozano AM, Voon V, McNeely HE, Seminowicz D, Hamani C, *et al.* (2005): Deep brain stimulation for treatment-resistant depression. *Neuron* 45:651–660.
5. Schlaepfer TE, Cohen MX, Frick C, Kosel M, Brodesser D, Axmacher N, *et al.* (2008): Deep brain stimulation to reward circuitry alleviates anhedonia in refractory major depression. *Neuropsychopharmacology* 33:368–377.
6. Bewernick BH, Hurlemann R, Matusch A, Kayser S, Grubert C, Hadrysiewicz B, *et al.* (2010): Nucleus accumbens deep brain stimulation decreases ratings of depression and anxiety in treatment-resistant depression. *Biol Psychiatry* 67:110–116.
7. Sartorius A, Kiening KL, Kirsch P, von Gall CC, Haberkorn U, Unterberg AW, *et al.* (2010): Remission of major depression under deep brain stimulation of the lateral habenula in a therapy-refractory patient. *Biol Psychiatry* 67:e9–e11.
8. Mayberg HS (2003): Modulating dysfunctional limbic-cortical circuits in depression: Towards development of brain-based algorithms for diagnosis and optimised treatment. *Br Med Bull* 65:193–207.
9. Mayberg HS, Liotti M, Brannan SK, McGinnis S, Mahurin RK, Jerabek PA, *et al.* (1999): Reciprocal limbic-cortical function and negative mood: Converging PET findings in depression and normal sadness. *Am J Psychiatry* 156:675–682.
10. Seminowicz DA, Mayberg HS, McIntosh AR, Goldapple K, Kennedy S, Segal Z, *et al.* (2004): Limbic-frontal circuitry in major depression: A path modeling metanalysis. *Neuroimage* 22:409–418.
11. Crossman AR (2005): Cerebral hemisphere. In: Standring S, editor. *Gray's Anatomy: The Anatomical Basis of Clinical Practice, 39th ed.* Edinburgh, London, New York, Oxford, Philadelphia, St Louis, Sidney, Toronto: Elsevier, Churchill, Livingstone, 387–417.
12. Devinsky O, Morrell MJ, Vogt BA (1995): Contributions of anterior cingulate cortex to behaviour. *Brain* 118:279–306.
13. Paus T (2001): Primate anterior cingulate cortex: Where motor control, drive and cognition interface. *Nat Rev Neurosci* 2:417–424.
14. Vogt BA (1993): Structural organization of cingulate cortex: Areas, neurons, and somatodendritic transmitter receptors. In: Vogt B, Gabriel M, editors. *Neurobiology of the Cingulate Cortex and Limbic Thalamus: A Comprehensive Handbook*. Boston/Basel/Berlin: Birkhäuser, 19–70.
15. Vogt BA (2005): Pain and emotion interactions in subregions of the cingulate gyrus. *Nat Rev Neurosci* 6:533–544.
16. Vogt BA, Vogt L, Farber NB, Bush G (2005): Architecture and neurocytology of monkey cingulate gyrus. *J Comp Neurol* 485:218–239.
17. Vogt B (2009): *Cingulate Neurobiology and Disease*. New York: Oxford University Press.
18. Ongur D, Ferry AT, Price JL (2003): Architectonic subdivision of the human orbital and medial prefrontal cortex. *J Comp Neurol* 460:425–449.
19. Vogt BA, Nimchinsky EA, Vogt LJ, Hof PR (1995): Human cingulate cortex: Surface features, flat maps, and cytoarchitecture. *J Comp Neurol* 359:490–506.
20. Vogt BA, Pandya DN (1987): Cingulate cortex of the rhesus monkey. II. Cortical afferents. *J Comp Neurol* 262:271–289.
21. Vogt BA, Pandya DN, Rosene DL (1987): Cingulate cortex of the rhesus monkey. I. Cytoarchitecture and thalamic afferents. *J Comp Neurol* 262: 256–270.
22. Gabbott PL, Bacon SJ (1996): Local circuit neurons in the medial prefrontal cortex (areas 24a,b,c, 25 and 32) in the monkey. II. Quantitative areal and laminar distributions. *J Comp Neurol* 364:609–636.
23. Gabbott PL, Bacon SJ (1996): Local circuit neurons in the medial prefrontal cortex (areas 24a,b,c, 25 and 32) in the monkey. I. Cell morphology and morphometrics. *J Comp Neurol* 364:567–608.
24. Nimchinsky EA, Vogt BA, Morrison JH, Hof PR (1997): Neurofilament and calcium-binding proteins in the human cingulate cortex. *J Comp Neurol* 384:597–620.
25. Palomero-Gallagher N, Vogt BA, Schleicher A, Mayberg HS, Zilles K (2009): Receptor architecture of human cingulate cortex: Evaluation of the four-region neurobiological model. *Hum Brain Mapp* 30:2336–2355.
26. Ongur D, Price JL (2000): The organization of networks within the orbital and medial prefrontal cortex of rats, monkeys and humans. *Cereb Cortex* 10:206–219.
27. Barbas H, Pandya DN (1989): Architecture and intrinsic connections of the prefrontal cortex in the rhesus monkey. *J Comp Neurol* 286:353–375.
28. Carmichael ST, Price JL (1996): Connectional networks within the orbital and medial prefrontal cortex of macaque monkeys. *J Comp Neurol* 371: 179–207.
29. Price JL, Carmichael ST, Drevets WC (1996): Networks related to the orbital and medial prefrontal cortex; a substrate for emotional behavior? *Prog Brain Res* 107:523–536.
30. Petrides M, Pandya DN (2007): Efferent association pathways from the rostral prefrontal cortex in the macaque monkey. *J Neurosci* 27:11573–11586.
31. Kondo H, Saleem KS, Price JL (2003): Differential connections of the temporal pole with the orbital and medial prefrontal networks in macaque monkeys. *J Comp Neurol* 465:499–523.
32. Pandya DN, Kuypers HG (1969): Cortico-cortical connections in the rhesus monkey. *Brain Res* 13:13–36.
33. Barbas H, Blatt GJ (1995): Topographically specific hippocampal projections target functionally distinct prefrontal areas in the rhesus monkey. *Hippocampus* 5:511–533.
34. Rosene DL, Van Hoesen GW (1977): Hippocampal efferents reach widespread areas of cerebral cortex and amygdala in the rhesus monkey. *Science* 198:315–317.
35. Amaral DG, Price JL (1984): Amygdalo-cortical projections in the monkey (*Macaca fascicularis*). *J Comp Neurol* 230:465–496.
36. Barbas H, De Olmos J (1990): Projections from the amygdala to basoventral and mediodorsal prefrontal regions in the rhesus monkey. *J Comp Neurol* 300:549–571.
37. Kondo H, Saleem KS, Price JL (2005): Differential connections of the perirhinal and parahippocampal cortex with the orbital and medial prefrontal networks in macaque monkeys. *J Comp Neurol* 493:479–509.
38. Ray JP, Price JL (1993): The organization of projections from the mediodorsal nucleus of the thalamus to orbital and medial prefrontal cortex in macaque monkeys. *J Comp Neurol* 337:1–31.

39. Dermon CR, Barbas H (1994): Contralateral thalamic projections predominantly reach transitional cortices in the rhesus monkey. *J Comp Neurol* 344:508–531.
40. Hsu DT, Price JL (2007): Midline and intralaminar thalamic connections with the orbital and medial prefrontal networks in macaque monkeys. *J Comp Neurol* 504:89–111.
41. Rempel-Clower NL, Barbas H (1998): Topographic organization of connections between the hypothalamus and prefrontal cortex in the rhesus monkey. *J Comp Neurol* 398:393–419.
42. Veazey RB, Amaral DG, Cowan WM (1982): The morphology and connections of the posterior hypothalamus in the cynomolgus monkey (*Macaca fascicularis*). I. Cytoarchitectonic organization. *J Comp Neurol.* 207: 114–134.
43. Gaspar P, Stepniewska I, Kaas JH (1992): Topography and collateralization of the dopaminergic projections to motor and lateral prefrontal cortex in owl monkeys. *J Comp Neurol* 325:1–21.
44. Goldman-Rakic PS, Lidow MS, Smiley JF, Williams MS (1992): The anatomy of dopamine in monkey and human prefrontal cortex. *J Neural Transm Suppl* 36:163–177.
45. Chiba T, Kayahara T, Nakano K (2001): Efferent projections of infralimbic and prelimbic areas of the medial prefrontal cortex in the Japanese monkey, *Macaca fuscata*. *Brain Res* 888:83–101.
46. Freedman LJ, Insel TR, Smith Y (2000): Subcortical projections of area. 25 (subgenual cortex) of the macaque monkey. *J Comp Neurol* 421:172–188.
47. Haber SN, Kim KS, Mailly P, Calzavara R (2006): Reward-related cortical inputs define a large striatal region in primates that interface with associative cortical connections, providing a substrate for incentive-based learning. *J Neurosci* 26:8368–8376.
48. Haber SN, Kunishio K, Mizobuchi M, Lynd-Balta E (1995): The orbital and medial prefrontal circuit through the primate basal ganglia. *J Neurosci* 15:4851–4867.
49. Ongur D, An X, Price JL (1998): Prefrontal cortical projections to the hypothalamus in macaque monkeys. *J Comp Neurol* 401:480–505.
50. Bachevalier J, Meunier M, Lu MX, Ungerleider LG (1997): Thalamic and temporal cortex input to medial prefrontal cortex in rhesus monkeys. *Exp Brain Res* 115:430–444.
51. Barbas H, Henion TH, Dermon CR (1991): Diverse thalamic projections to the prefrontal cortex in the rhesus monkey. *J Comp Neurol* 313:65–94.
52. Ferry AT, Ongur D, An X, Price JL (2000): Prefrontal cortical projections to the striatum in macaque monkeys: Evidence for an organization related to prefrontal networks. *J Comp Neurol* 425:447–470.
53. An X, Bandler R, Ongur D, Price JL (1998): Prefrontal cortical projections to longitudinal columns in the midbrain periaqueductal gray in macaque monkeys. *J Comp Neurol* 401:455–479.
54. Frankle WG, Laruelle M, Haber SN (2006): Prefrontal cortical projections to the midbrain in primates: Evidence for a sparse connection. *Neuropsychopharmacology* 31:1627–1636.
55. Damasio AR, Grabowski TJ, Bechara A, Damasio H, Ponto LL, Parvizi J, *et al.* (2000): Subcortical and cortical brain activity during the feeling of self-generated emotions. *Nat Neurosci* 3:1049–1056.
56. George MS, Ketter TA, Parekh PI, Horwitz B, Herscovitch P, Post RM (1995): Brain activity during transient sadness and happiness in healthy women. *Am J Psychiatry* 152:341–351.
57. Pardo JV, Pardo PJ, Raichle ME (1993): Neural correlates of self-induced dysphoria. *Am J Psychiatry* 150:713–719.
58. Talbot PS, Cooper SJ (2006): Anterior cingulate and subgenual prefrontal blood flow changes following tryptophan depletion in healthy males. *Neuropsychopharmacology* 31:1757–1767.
59. Dougherty DD, Weiss AP, Cosgrove GR, Alpert NM, Cassem EH, Nierenberg AA, *et al.* (2003): Cerebral metabolic correlates as potential predictors of response to anterior cingulotomy for treatment of major depression. *J Neurosurg* 99:1010–1017.
60. Drevets WC, Price JL, Simpson JR Jr, Todd RD, Reich T, Vannier M, *et al.* (1997): Subgenual prefrontal cortex abnormalities in mood disorders. *Nature* 386:824–827.
61. Konarski JZ, Kennedy SH, Segal ZV, Lau MA, Bieling PJ, McIntyre RS, *et al.* (2009): Predictors of nonresponse to cognitive behavioural therapy or venlafaxine using glucose metabolism in major depressive disorder. *J Psychiatry Neurosci* 34:175–180.
62. George MS, Stallings LE, Speer AM, Nahas Z, Spicer KM, Vincent DJ, *et al.* (1999): Prefrontal repetitive transcranial magnetic stimulation (rTMS) changes relative perfusion locally and remotely. *Hum Psychopharmacol Clin Exp* 14:161–170.
63. Mayberg HS, Silva JA, Brannan SK, Tekell JL, Mahurin RK, McGinnis S, *et al.* (2002): The functional neuroanatomy of the placebo effect. *Am J Psychiatry* 159:728–737.
64. Mottaghy FM, Keller CE, Gangitano M, Ly J, Thall M, Parker JA, *et al.* (2002): Correlation of cerebral blood flow and treatment effects of repetitive transcranial magnetic stimulation in depressed patients. *Psychiatry Res* 115:1–14.
65. Nobler MS, Oquendo MA, Kegeles LS, Malone KM, Campbell CC, Sackeim HA, *et al.* (2001): Decreased regional brain metabolism after ETC. *Am J Psychiatry* 158:305–308.
66. Harrison PJ (2002): The neuropathology of primary mood disorder. *Brain* 125:1428–1449.
67. Rajkowska G (2000): Postmortem studies in mood disorders indicate altered numbers of neurons and glial cells. *Biol Psychiatry* 48:766–777.
68. Rajkowska G (2002): Cell pathology in mood disorders. *Semin Clin Neuropsychiatry* 7:281–292.
69. Rajkowska G (2003): Depression: What we can learn from postmortem studies. *Neuroscientist* 9:273–284.
70. Rajkowska G, Miguel-Hidalgo JJ, Wei J, Dilley G, Pittman SD, Meltzer HY, *et al.* (1999): Morphometric evidence for neuronal and glial prefrontal cell pathology in major depression. *Biol Psychiatry* 45:1085–1098.
71. Ongur D, Drevets WC, Price JL (1998): Glial reduction in the subgenual prefrontal cortex in mood disorders. *Proc Natl Acad Sci U S A* 95:13290–13295.
72. Banasr M, Duman RS (2008): Glial loss in the prefrontal cortex is sufficient to induce depressive-like behaviors. *Biol Psychiatry* 64:863–870.
73. Banasr M, Chowdhury GM, Terwilliger R, Newton SS, Duman RS, Behar KL, *et al.* (2008): Glial pathology in an animal model of depression: Reversal of stress-induced cellular, metabolic and behavioral deficits by the glutamate-modulating drug riluzole. *Mol Psychiatry* 15:501–11.
74. Jansson L, Wennstrom M, Johanson A, Tingstrom A (2009): Glial cell activation in response to electroconvulsive seizures. *Prog Neuropsychopharmacol Biol Psychiatry* 33:1119–1128.
75. Ongur D, Pohlman J, Dow AL, Eisch AJ, Edwin F, Heckers S, *et al.* (2007): Electroconvulsive seizures stimulate glial proliferation and reduce expression of Sprouty2 within the prefrontal cortex of rats. *Biol Psychiatry* 62:505–512.
76. Botteron KN, Raichle ME, Drevets WC, Heath AC, Todd RD (2002): Volumetric reduction in left subgenual prefrontal cortex in early onset depression. *Biol Psychiatry* 51:342–344.
77. Coryell W, Nopoulos P, Drevets W, Wilson T, Andreasen NC (2005): Subgenual prefrontal cortex volumes in major depressive disorder and schizophrenia: Diagnostic specificity and prognostic implications. *Am J Psychiatry* 162:1706–1712.
78. Sharma V, Menon R, Carr TJ, Densmore M, Mazmanian D, Williamson PC (2003): An MRI study of subgenual prefrontal cortex in patients with familial and non-familial bipolar I disorder. *J Affect Disord* 77: 167–171.
79. Brambilla P, Nicoletti MA, Harenski K, Sassi RB, Mallinger AG, Frank E, *et al.* (2002): Anatomical MRI study of subgenual prefrontal cortex in bipolar and unipolar subjects. *Neuropsychopharmacology* 27:792–799.
80. Pezawas L, Meyer-Lindenberg A, Drabant EM, Verchinski BA, Munoz KE, Kolachana BS, *et al.* (2005): 5-HTTLPR polymorphism impacts human cingulate-amygdala interactions: A genetic susceptibility mechanism for depression. *Nat Neurosci* 8:828–834.
81. Saper CB, Scammell TE, Lu J (2005): Hypothalamic regulation of sleep and circadian rhythms. *Nature* 437:1257–1263.
82. Drevets WC (1999): Prefrontal cortical-amygdalar metabolism in major depression. *Ann N Y Acad Sci* 877:614–637.
83. Sheline YI, Barch DM, Donnelly JM, Ollinger JM, Snyder AZ, Mintun MA (2001): Increased amygdala response to masked emotional faces in depressed subjects resolves with antidepressant treatment: An fMRI study. *Biol Psychiatry* 50:651–658.
84. Mayberg HS, Brannan SK, Tekell JL, Silva JA, Mahurin RK, McGinnis S, *et al.* (2000): Regional metabolic effects of fluoxetine in major depression: Serial changes and relationship to clinical response. *Biol Psychiatry* 48: 830–843.
85. McNeely HE, Mayberg HS, Lozano AM, Kennedy SH (2008): Neuropsychological impact of Cg25 deep brain stimulation for treatment-resistant depression: Preliminary results over 12 months. *J Nerv Ment Dis* 196:405–410.

86. Hamani C, Diwan M, Isabella S, Lozano AM, Nobrega JN (2010): Effects of different stimulation parameters on the antidepressant-like response of medial prefrontal cortex deep brain stimulation in rats. *J Psychiatr Res* 44:683–687.
87. Hamani C, Diwan M, Macedo CE, Brandao ML, Shumake J, Gonzalez-Lima F, *et al.* (2010): Antidepressant-like effects of medial prefrontal cortex deep brain stimulation in rats. *Biol Psychiatry* 67:117–124.
88. Hamani C, Dubiela FP, Soares JC, Shin D, Bittencourt S, Covolan L, *et al.* (2010): Anterior thalamus deep brain stimulation at high current impairs memory in rats. *Exp Neurol* 225:154–162.
89. Lozano AM, Dostrovsky J, Chen R, Ashby P (2002): Deep brain stimulation for Parkinson's disease: Disrupting the disruption. *Lancet Neurol* 1:225–231.
90. Slattery DA, Neumann I, Cryan JF (2010): Transient inactivation of the infralimbic cortex induces antidepressant-like effects in the rat [published online ahead of print June 8]. *J Psychopharmacol*.
91. Hamani C, Nobrega JN (2010): Deep brain stimulation in an animal model of depression. *Eur J Neurosci* 32:1109–1117.
92. Hamani C, Mayberg H, Snyder B, Giacobbe P, Kennedy S, Lozano AM (2009): Deep brain stimulation of the subcallosal cingulate gyrus for depression: Anatomical location of active contacts in clinical responders and a suggested guideline for targeting. *J Neurosurg* 111:1209–1215.
93. Vitek JL (2002): Mechanisms of deep brain stimulation: Excitation or inhibition. *Mov Disord* 17(suppl 3):S69–S72.
94. Schmahmann JD, Pandya DN (2006): *Fiber Pathways of the Brain*. New York: Oxford Press.
95. Johansen-Berg H, Gutman DA, Behrens TE, Matthews PM, Rushworth MF, Katz E, *et al.* (2008): Anatomical connectivity of the subgenual cingulate region targeted with deep brain stimulation for treatment-resistant depression. *Cereb Cortex* 18:1374–1383.
96. Gutman DA, Holtzheimer PE, Behrens TE, Johansen-Berg H, Mayberg HS (2009): A tractography analysis of two deep brain stimulation white matter targets for depression. *Biol Psychiatry* 65:276–282.
97. Agid Y, Buzsáki G, Diamond DM, Frackowiak R, Giedd J, Girault JA, *et al.* (2007): How can drug discovery for psychiatric disorders be improved? *Nat Rev Drug Discov* 6:189–201.